

# 1 The impact of spray mediated enhanced enthalpy and reduced 2 drag coefficients in modelling of tropical cyclones

3 N.C. Zweers<sup>‡</sup>, V.K. Makin, J.W. de Vries

4 *Royal Netherlands Meteorological Institute (KNMI), De Bilt, The Netherlands*

5 V.N. Kudryavtsev

6 *Nansen International Environmental and Remote Sensing Centre (NIERSC), Saint*

7 *Petersburg, Russia*

8 *Russian State Hydrometeorological University (RSU), Saint Petersburg, Russia*

9 **Abstract.** The impact of new parametrizations for drag and air-sea enthalpy exchange on  
10 modelling the intensity of tropical cyclones with a numerical weather prediction (NWP) model  
11 is examined. These parameterizations follow from a model for the marine atmospheric bound-  
12 ary layer (MABL) for high wind speed conditions in the presence of spray droplets that  
13 originate from breaking wave crests. This model accounts for the direct impact of these  
14 droplets on the air-sea momentum flux through action of a *spray force*, which originates from  
15 the interaction of the ‘rain’ of spray droplets with the vertical wind shear and is expressed  
16 in terms of the spray generation function (SGF). The SGF is cubic in the wind speed up to  
17  $50 \text{ m s}^{-1}$  beyond which its value increases less strongly. The drag coefficient ( $C_D$ ) decreases  
18 from approximately  $30 \text{ m s}^{-1}$ , as in agreement with what the available measurements in these  
19 conditions indicate. The enthalpy exchange coefficient ( $C_k$ ) increases with increasing wind  
20 speed and slowly decreases beyond a wind speed of about  $40 \text{ m s}^{-1}$  due to the strong drop  
21 in  $C_D$ . The value for  $C_k/C_D$  is in agreement with observational data for wind speeds up to  $30$   
22  $\text{m s}^{-1}$ ; for higher wind speeds the value is in the range 1.2–1.5 as in agreement with a well  
23 established theory. The parametrization is tested in an NWP model. The tropical cyclones Ivan  
24 (2004) and Katrina (2005) in the Gulf of Mexico are simulated. To the sea surface tempera-  
25 tures (SSTs) from the European Centre archive that were prescribed to the NWP model, a  
26 parametrized cooling (based on estimations from theoretical studies and measurements) was  
27 applied during the model forecasts, as the NWP model does not resolve locally rather strong  
28 induced reductions in SSTs. The simulations show that realistic tropical cyclone wind speeds  
29 and central pressure can be obtained with the proposed drag and enthalpy parametrization.  
30 The results indicate that the value for  $C_k/C_D$  at very high wind speeds in this study is in  
31 the correct range. Moreover, the results motivate the application of the parametrizations in  
32 atmosphere–ocean coupled models.

33 **Keywords:** Drag Coefficient, Enthalpy Exchange Coefficient, High Wind Speeds, Spray, Trop-  
34 ical Cyclones

## 35 1. Introduction

36 One of the challenges in tropical cyclone modelling is understanding and  
37 representing the physical processes near the sea surface that determine the  
38 surface fluxes of latent and sensible heat, and momentum. Tropical cyclones,  
39 also known as hurricanes, gain their intensity from the warm ocean through  
40 exchange of heat and moisture, while momentum is exchanged through the



<sup>‡</sup> Current affiliation: MeteoGroup, Wageningen, The Netherlands

© 2014 Kluwer Academic Publishers. Printed in the Netherlands.

41 drag that is exerted on the atmospheric flow. Numerical weather prediction  
 42 (NWP) models normally compute the air-sea fluxes of momentum  $\tau$ , sensi-  
 43 ble heat  $H_S$  and latent heat  $H_E$  with a bulk type relation with an exchange  
 44 coefficient according to,

$$\tau = \rho_a C_D U_L^2, \quad (1)$$

$$H_S = \rho_a c_p C_H U_L (\theta_0 - \theta_L), \quad (2)$$

$$H_E = \rho_a L_v C_E U_L (q_0 - q_L), \quad (3)$$

47 with  $\rho_a$  the density of air,  $c_p$  the specific heat of air (at constant pressure),  
 48  $L_v$  the latent heat of vaporization, and  $U$ ,  $\theta$  and  $q$  are respectively the wind  
 49 speed, potential temperature and specific humidity, with subscript 0 the sur-  
 50 face and  $L$  a reference level height.  $C_H$  and  $C_E$  are the exchange coefficients  
 51 for respectively heat and moisture, and  $C_D$  is the drag coefficient.

52 For neutral stratification, the wind field in the marine atmospheric bound-  
 53 ary layer (MABL) in NWP models is assumed to be logarithmic with height.  
 54 Then,

$$C_D = \kappa^2 / [\ln^2 ((z + z_{0M}) / z_{0M})], \quad (4)$$

$$C_H = \kappa \sqrt{C_D} / [Pr_t \ln ((z + z_{0H}) / z_{0H})], \quad (5)$$

$$C_E = \kappa \sqrt{C_D} / [Pr_t \ln ((z + z_{0E}) / z_{0E})], \quad (6)$$

57 with  $\kappa$  (=0.40) the von Karman constant,  $z$  the height above the sea surface,  
 58  $Pr_t$  the turbulent Prandtl number, and  $z_{0M}$ ,  $z_{0H}$ ,  $z_{0E}$  the roughness lengths for  
 59 momentum, heat and moisture, respectively.

60 As suggested by Emanuel (1986) and Emanuel (1995), the intensity of  
 61 tropical cyclones in atmospheric models strongly depends on the ratio of the  
 62 exchange coefficients for enthalpy  $C_k$  and momentum  $C_D$ . Here,  $C_k$  can be  
 63 obtained from the enthalpy flux  $H_k$ , which corresponds to specific enthalpy  $k$   
 64  $= c_p \theta + L_v q$ , according to

$$H_k = \rho_a C_k U_L (k_0 - k_L). \quad (7)$$

65 Emanuel (1995) concluded that  $C_k/C_D$  should be in the range 1.2–1.5, in  
 66 order to model realistic tropical cyclone intensity, with 0.75 as a lower bound.  
 67 Measurement data in the tropical cyclone boundary layer are still limited.  
 68 Hence, there is still a rather large gap in understanding what happens at the  
 69 sea surface. The behaviour of  $C_H$ ,  $C_E$  and  $C_D$  are still studied. Analyses by  
 70 Powell et al. (2003) of measurements with Global Positioning System (GPS)  
 71 drop sondes show that the magnitude of  $C_D$  starts to decrease from a wind  
 72 speed of 30–40 m s<sup>-1</sup>. Analyses of Holthuijsen et al. (2012), which show  
 73 a dependence of  $C_D$  to the different azimuthal angles in tropical cyclones,  
 74 confirm in general the findings by Powell. Analyses by Jarosz et al. (2007) of  
 75 buoy data measuring ocean currents show a similar behaviour for  $C_D$  at very  
 76 high wind speeds.

77 Different reasons for a possible reduction in the drag at high wind speeds  
78 have been suggested. Makin (2005), Bye and Jenkins (2006), Kudryavtsev  
79 (2006) and Rastigejev et al. (2011), speculate on the impact of spray droplets,  
80 as suspended particles, on atmospheric stratification. Within the frame of  
81 this ‘stratification mechanism’, however, the observed suppression of the sea  
82 drag can only be attained at an unrealistically large volume concentration  
83 ( $\mathcal{O}(10^{-3})$  or even larger) of sea spray (e.g. Kudryavtsev (2006), Rastigejev  
84 et al. (2011)). Another cause is the direct impact of droplets on the momentum  
85 balance through ‘spray stress’ (or ‘spray force’). As illustrated by Andreas  
86 (2004) and Kudryavtsev and Makin (2011) this should be a more efficient  
87 way than through stratification. In addition, foam and streaks (of foam and  
88 spray) are suggested as a cause as well (Powell et al. (2003), Holthuijsen  
89 et al. (2012)).

90 The impact of reduced drag at high wind speeds on modelling tropical  
91 cyclone intensity has been examined by Zweers et al. (2010). They simu-  
92 late severe tropical cyclones with reduced  $C_D$ , while their monotonically  
93 increasing drag coefficient results in significantly lower wind speeds.

94 The available measurement data are also questioned. Smith and Mont-  
95 gomery (2014) question the assumption of a logarithmic wind profile at very  
96 high wind speeds that Powell uses for computing  $C_D$ . Moon et al. (2007),  
97 who propose an empirical  $C_D$  based on previous numerical calculations with  
98 a coupled atmospheric-wave model, suggest that  $C_D$  saturates at very high  
99 wind speeds. Their  $C_D$  shows poor agreement with available measurement  
100 data. In general, Richter and Sullivan (2013) mention that only the turbulent  
101 stress above the sea surface is measured at very high wind speeds. Therefore,  
102 the turbulent drag would decrease, but the atmospheric drag starts to saturate.

103  
104 Analyses of CBLAST data by Zhang et al. (2008) indicate that with “95%  
105 confidence”  $C_H = C_E = C_k$  for wind speeds up to about  $30 \text{ m s}^{-1}$ . Using  
106 momentum flux measurements by French et al. (2007), they show that  $<$   
107  $C_k/C_D >=0.63$ , which is smaller than Emanuel’s critical value of 0.75. Zhang  
108 et al. (2008) speculate that “the enthalpy flux into the hurricane boundary  
109 layer may have come from sources other than air-sea turbulent fluxes, or the  
110 Emanuel model assumptions should be revisited”. Andreas (2011) mentions  
111 Emanuel’s criterion is often misinterpreted: for tropical cyclone wind speeds  
112  $C_k/C_D < 0.75$ , while its value might be smaller for lower wind speeds. While  
113  $C_k/C_D$  obtained from Andreas’ algorithm shows agreement with Emanuel’s  
114 favourable range of 1.2–1.5 in the high wind speed regime,  $C_D$  keeps increas-  
115 ing monotonically with increasing wind speed, which is not what available  
116 measurement data suggest:  $C_D$  would start to reduce.

117  
118 In the present study the impact of an air-sea exchange parametrization on  
119 modelling tropical cyclone intensity with an NWP model is examined. The

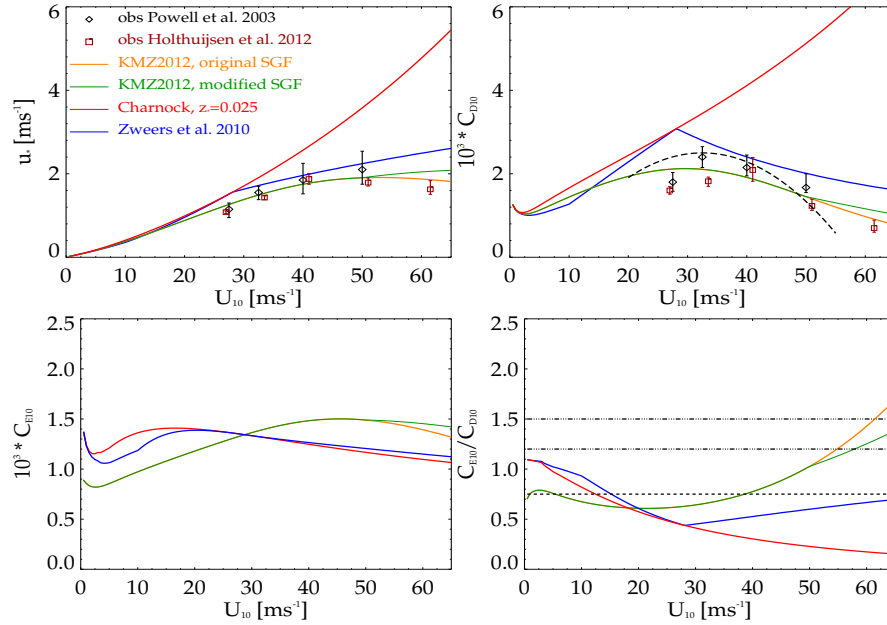


Figure 1. Friction velocity  $u_*$  (top left), 10 m drag coefficient  $C_{D10}$  (top right), 10 m humidity exchange coefficient  $C_{E10}$  (bottom left), and ratio  $C_{E10}/C_{D10}$  (bottom right) versus 10 m wind speed  $U_{10}$ , according to different parametrizations (see legend; KMZ2012 refers to Kudryavtsev et al. (2012)); observations are in black (Powell et al., 2003) and brown (Holthuijsen et al., 2012); the dashed black curve for  $C_{D10}$  is from Jarosz et al. (2007); range for  $C_{E10}/C_{D10}$  suggested by Emanuel (1995) in black dashed-dotted lines with the black dashed line is the 0.75 lower bound.

120 parametrization is based on the model by Kudryavtsev and Makin (2011),  
 121 in which the impact of spray droplets on the momentum flux is directly ac-  
 122 counted for in the way of a spray stress ('vortex force'). The model produces  
 123 a decrease in the drag at very high wind speeds, as in agreement with the  
 124 available measurements in these conditions. In the model, further explored by  
 125 Kudryavtsev et al. (2012), the air-sea enthalpy transfer is enhanced. Hence,  
 126 the parametrized reduced  $C_D$  and enhanced  $C_k$  from Kudryavtsev et al. (2012)  
 127 are tested. The parametrizations are used in the NWP model HiRLAM<sup>1</sup> (High  
 128 Resolution Limited Area Model) to simulate the tropical cyclones Ivan (2004)  
 129 and Katrina (2005) in the Gulf of Mexico. The reduction in the drag, and also  
 130 the increase in  $C_k$ , is based on a different physical mechanism than in e.g.  
 131 Zweers et al. (2010).

132 The outline is as follows. In Section 2 we present the parametrizations for  
 133  $C_k$  and  $C_D$  that are tested and explain on the simulations performed with the  
 134 NWP model. Results are presented in Section 3, followed by a concluding  
 135 section.

<sup>1</sup> see <http://www.hirlam.org/> for more information on HiRLAM

136

## 2. Methods

137 A different air-sea exchange scheme is applied than Zweers et al. (2010) have  
 138 used. They compute  $C_H$  and  $C_E$  in HiRLAM with formulations for  $z_{0H}$  and  
 139  $z_{0E}$  based on extrapolation of the empirical formulations proposed by Garratt  
 140 (1992):

$$\ln \frac{z_{0M}}{z_{0H}} = 2.48 Re_*^{1/4} - 2, \quad (8)$$

141

$$\ln \frac{z_{0M}}{z_{0E}} = \ln \frac{z_{0M}}{z_{0H}} - 0.2 Re_*^{1/4}, \quad (9)$$

142 with  $Re_* = z_{0M} u_* / \nu$  the Reynolds number, with  $u_* = \sqrt{\tau / \rho_a}$  the friction  
 143 velocity and  $\nu$  the molecular kinematic viscosity of air. The behaviour of and  
 144 the values for the exchange coefficients  $C_H$  and  $C_E$  are quite similar with  
 145 (8) and (9). A change in the drag comes with changes in the exchange of  
 146 heat and moisture. This is in fact a natural consequence (see Section 2.1).  
 147 But with (8) and (9) these changes are not dramatic (see Figure 1). The drag  
 148 parametrization by Zweers et al. (2010) together with (8) and (9) gives values  
 149 for  $C_E/C_D$  (or  $C_H/C_D$ ) that are below Emanuel's critical value of 0.75 for all  
 150 (high) wind speeds (see Figure 1).

151 In the present study (8) and (9) are not used. Here,  $C_D$  is reduced more  
 152 severely and  $C_k$  is enhanced more strongly. A description is given in the next  
 153 paragraph.

### 2.1. DRAG AND ENTHALPY EXCHANGE COEFFICIENT

154  
 155 At very high wind speeds the airflow near the air-sea interface is heavily  
 156 loaded with spray droplets. In these conditions, the use of traditional equa-  
 157 tions for the MABL dynamics is not justified. Therefore, Kudryavtsev and  
 158 Makin (2011) (hereinafter KM2011) derived equations in which spray effects  
 159 on the MABL dynamics are directly accounted for. KM2011 used a modified  
 160 form of the mass and momentum conservation equations that take into ac-  
 161 count the injection of droplets into the airflow at the height of breaking wave  
 162 crests. In the momentum conservation equation they included the volume  
 163 source of the droplet momentum. This is the rate of injection of momentum  
 164 of the droplets, that are torn off from breaking wave crests, in a unit volume  
 165 of air at height  $z$  (see eq. (8) in KM2011).

166 Kudryavtsev et al. (2012) (hereinafter KMZ2012) present a simplified  
 167 model (parametrizations) for the MABL that is based on the model by KM2011.  
 168 In the present study the impact of these parametrizations on modelling tropi-  
 169 cal cyclone intensity is investigated. For a full and detailed description of  
 170 the model and the parametrizations we refer to the original papers; here, we  
 171 briefly present and explain the parametrizations.

172 The simplified model by KMZ2012 is a two layer model in which the  
173 MABL consists of a thin layer adjacent to the sea surface in which spray  
174 droplets are generated from breaking wave crests – the spray generation layer  
175 (SGL) – and the core of the MABL above the SGL. The spectral distribution  
176 of wave breaking parameters (e.g. length of breaking fronts, or distribution of  
177 white caps over wavenumbers) rapidly grows towards high wavenumbers, as  
178 suggested by Phillips (1985). This is why in the KMZ2012 model the SGL  
179 (associated with spume droplets generation) is a relatively shallow layer with  
180 depth  $d$  that is proportional to the inverse wavenumber of shortest breaking  
181 waves  $k_b$  that carry white caps ( $k_b \simeq 10 \text{ rad m}^{-1}$ ). These rather short breaking  
182 waves are strongly modulated by large dominant wind waves. Hence, the pro-  
183 duction of spume droplets largely takes place on top of the dominant waves  
184 and on their crests, as is discussed in Kudryavtsev and Makin (2009).

185 In the model by KMZ2012 the droplets act on the airflow dynamics through  
186 the ‘spray force’. The interpretation of this mechanism is the following. At  
187 moderate and high wind speeds the surface stress is fully supported by the  
188 surface form drag. At higher wind speeds the crests of breaking waves can be  
189 disrupted aerodynamically (e.g. by Kelvin-Helmholtz type instability) and  
190 they are pulverized to droplets. The physical meaning of the mechanism  
191 suggested in KM2011 is that the form drag, initially supported by the wave  
192 crests, is transferred to the droplets once these crests have been subjected to  
193 the aerodynamical disruption and fragmentation. The droplets are produced  
194 at the height of the breaking crests.

195 Once generated, the droplets are embedded in the airflow, following the  
196 streamlines of the dominant waves. The droplets stay relatively close to the  
197 sea surface, as the airflow does not separate from the dominant waves. While  
198 falling back to the sea surface, the droplets transfer momentum to the airflow.  
199 Hence, the turbulent stress in the SGL increases and droplets will accelerate  
200 the airflow near the surface. As a result of this acceleration, in the core of the  
201 MABL (above the SGL) the vertical wind shear reduces and turbulence will  
202 be suppressed. This results in a reduction in the drag coefficient in the core of  
203 the MABL. Thus, while inside the SGL the turbulent mixing of momentum  
204 is enhanced, it is suppressed above the SGL. And the combination of aero-  
205 dynamic disruption of wave crests (that initially provided the form drag) and  
206 injection of droplets into the airflow represents a coupled process that results  
207 into acceleration of the airflow and suppression of the sea drag at high wind  
208 speeds.

209 Furthermore, due to the enhanced turbulent mixing inside the SGL, spray  
210 droplets enhance the turbulent exchange of heat and moisture. This leads  
211 to reduced vertical gradients of these quantities in the SGL. This can be  
212 understood by considering the small upward shift of the surface values of  
213 temperature and humidity to the depth of the SGL. As a result, the vertical  
214 gradients of humidity and heat are enhanced above the SGL. Hence, through

215 this mechanism spray droplets enhance the exchange of latent and sensible  
216 heat in the core of the MABL in this model.

217

218 A logarithmic wind profile is assumed. Then, the drag coefficient at height  
219  $h$  can be written as

$$C_{Dh} = \kappa^2 [\ln(h/Z_{0M})]^{-2}. \quad (10)$$

220 Following KMZ2012, we write the effective roughness length for momentum,  
221  $Z_{0M}$ , as

$$Z_{0M} = z_0 \exp(-\Delta_m). \quad (11)$$

222 For near-surface wind speeds up to approximately  $30 \text{ m s}^{-1}$  the effective  
223 roughness length is equal to the aerodynamic roughness,  $z_0$ , which is com-  
224 puted with Charnock's relation ((Charnock, 1955))

$$z_0 = z_* u_*^2 / g, \quad (12)$$

225 in which  $z_*$  is the dimensionless aerodynamic roughness length, or Charnock's  
226 parameter. With further increase in the wind speed  $Z_{0M}$  decreases due to  
227 the increasing impact of spray droplets on the MABL dynamics. This is  
228 represented by the function  $\Delta_m$ , which is determined by the spray genera-  
229 tion function (SGF). The SGF, denoted as  $\hat{F}_s(u_*, z)$ , determines the vertical  
230 profiles of spray and the wind. We assume that inside the SGL, the vertical  
231 distribution of  $\hat{F}_s(u_*, z)$  can be approximated by the spray flux at the surface,  
232 i.e.  $\hat{F}_s(u_*, z) = F_s^0(u_*)$ . KMZ2012 parametrize the SGF as

$$F_s^0 = c_s u_* (U_{10}/c_b)^3, \quad (13)$$

233 with  $U_{10}$  the wind speed at 10 m height,  $c_s$  a constant ( $\simeq 10^{-9}$ ) and  $c_b$  the  
234 phase velocity of the shortest breaking waves that produce droplets ( $c_b \simeq$   
235  $0.63 \text{ m s}^{-1}$ ). Note that KM2011 compute the total length of wave breaking  
236 fronts, which is cubic in the wind speed. This quantity is included here in  
237 terms of  $(U_{10}/c_b)^3$ . The function  $\Delta_m$  then depends on  $F_s^0$  through

$$\Delta_m = c_m (U_{10}/c_b)^3 = c_m F_s^0 / u_* c_s, \quad (14)$$

238 with  $c_m \simeq 10^{-6}$  a function that weakly depends on  $u_*$ .

239 With formulation (13) the SGF rapidly grows with increasing wind speed.  
240 KMZ2012 show there is fair agreement between (13) and conditions observed  
241 in laboratory experiments at very high wind speeds (see their Figure 1). As  
242 Kudryavtsev (2006) speculates, though, at very high wind speeds the total  
243 length of wave breaking fronts should be saturated. This seems plausible,  
244 as the sea surface must have a limited configuration in those extreme con-  
245 ditions, when almost each individual wave crest will break. This implies  
246 that formulation (13) overestimates the production of spray droplets in these  
247 conditions.

248 Moreover, a visual indicator of wave breaking is white capping. Holthui-  
 249 jsen et al. (2012) report on the generation of streaks of foam and spray at very  
 250 high wind speeds. These streaks may originate from white caps and may also  
 251 merge with these white caps. Their analysis and photographic evidence show  
 252 that the white cap coverage remains almost constant from a wind speed of  
 253 about  $40 \text{ m s}^{-1}$ . Formulation (13) leads to a decrease in the friction velocity  
 254 and very low values for  $C_D$  (see Figure 1, orange lines) at very high wind  
 255 speeds;  $C_D$  seems to drop even below the viscous drag. This implies that  
 256 almost all the white caps are pulverized into droplets. That is in contradiction  
 257 with the observed convergence in the degree of white capping mentioned  
 258 above.

259 In the present study the rapid increase in the droplet production and the  
 260 very strong drop in  $C_D$  at very high wind speeds is prevented through reduction  
 261 of the term  $(U_{10}/c_b)^3$  from a certain threshold wind speed  $U_T$ . Hence,  
 262 while relation (13) applies for  $U_{10} \leq U_T$ , for  $U_{10} > U_T$  we propose the fol-  
 263 lowing relation:

$$F_s^0 = c_s u_* (U_{10}/c_b)^2 (U_T/c_b). \quad (15)$$

264 The precise value for  $U_T$  may be a subject of future studies; here, we use  $U_T =$   
 265  $50 \text{ m s}^{-1}$ . With this modified SGF the friction velocity does not decrease  
 266 anymore at very high wind speeds, but it starts to saturate with increasing  
 267 wind speed (see Figure 1, green lines). Then, the dramatic drop in  $C_D$  at very  
 268 high wind speeds and the rapid growth in  $C_k/C_D$  is avoided (see Figure 1).

269 The exchange coefficients for humidity  $C_E$  and heat  $C_H$  are assumed equal.  
 270 This is based on extending the result by Zhang et al. (2008) to the hurricane  
 271 wind speed regime (see Section 1). Focusing on the humidity exchange co-  
 272 efficient  $C_E$ , we note that the formulations also apply for  $C_H$ . The humidity  
 273 exchange coefficient at height  $z = h$ , denoted as  $C_{Eh}$ , is computed as

$$C_{Eh} = \kappa^2 [Pr_t \ln(h/Z_{0E}) \ln(h/Z_{0M})]^{-1}, \quad (16)$$

274 which can also be written as

$$C_{Eh} = \frac{\kappa}{Pr_t \ln(h/Z_{0E})} \sqrt{C_{Dh}}. \quad (17)$$

275 The effective roughness lengths for humidity  $Z_{0E}$  (and temperature  $Z_{0H}$ )  
 276 used in this study do not take into account the impact of evaporation from  
 277 droplets on the moisture and heat balance. The droplets, which originate from  
 278 short breaking waves on top of large dominant waves (see Section 2.1), stay  
 279 close to the sea surface, follow the streamlines of these large dominant waves  
 280 and do not evaporate inside the SGL.

281 The effective roughness length for humidity, denoted as  $Z_{0E}$ , is parametrized  
 282 as

$$Z_{0E} = z_{0E} (d/z_{0E})^{(1-\ln(1+\Delta_E)/\Delta_E)}. \quad (18)$$



283 The value for  $Z_{0E}$  equals a constant background roughness length  $z_{0E}$  in case  
 284 there are no spray droplets, and grows with increasing wind speed towards  
 285 a value close to the depth of the SGL  $d$  ( $\simeq 0.1$  m), as a result of enhanced  
 286 turbulent mixing inside the SGL. This is represented in the parametrizations  
 287 by  $\Delta_E$ , which in a similar way depends on  $F_s^0$  as  $\Delta_m$ , according to

$$\Delta_E = c_E(U_{10}/c_b)^3 = c_E F_s^0 / u_* c_s, \quad (19)$$

288 with  $c_E \simeq 4.5 \times 10^{-6}$ .

289 The physical explanation for the parametrization in (18) is the following.  
 290 Spray droplets enhance the turbulent exchange of heat and moisture in the  
 291 SGL. This effect may seem to be inconsistent with suppression of the mo-  
 292 mentum exchange. However, such an effect has a clear physical meaning.  
 293 Within the frame of the wind-over-waves coupling theory, the heat exchange  
 294 coefficient is directly linked to the coupling parameter, which is the ratio of  
 295 the surface stress supported by the form drag to the total stress in the marine  
 296 atmospheric boundary layer (see e.g. Makin (1999)). At moderate and high  
 297 wind speeds the coupling parameter tends towards the value of 1. This has to  
 298 result in a rapid decrease of the roughness length for temperature ( $z_{0H}$ ) and  
 299 humidity ( $z_{0E}$ ). Empirical formulations such as e.g. (8) and (9) do describe  
 300 this effect: the values for  $z_{0E}$  and  $z_{0H}$  decrease with increasing wind speed.  
 301 When crests of breaking waves are pulverized to droplets at very high wind  
 302 speeds, the surface form drag is suppressed. This should inevitably result into  
 303 enhancement of the heat transfer. Hence, both mechanisms – the suppression  
 304 of the momentum exchange coefficient and the enhancement of the heat (and  
 305 humidity) exchange coefficient due to the generation of spray droplets – are  
 306 taken into account in the parametrizations by KMZ2012 that are tested here.

307 The humidity exchange coefficient depends on both  $Z_{0M}$  and  $Z_{0E}$  (see eq.  
 308 (16)). Due to the rapid growth of  $Z_{0E}$ ,  $C_{E10}$  still increases for wind speeds  
 309 larger than  $30 \text{ m s}^{-1}$ . For wind speeds larger than approximately  $40 \text{ m s}^{-1}$   
 310 the strong reduction in  $Z_{0M}$  starts to dominate the increase in  $Z_{0E}$ . Then,  $C_{E10}$   
 311 starts to decrease with further increase in the wind speed (see eq. (16)).

312 Figure 1 shows the friction velocity  $u_*$ , 10 m drag coefficient  $C_{D10}$ , 10 m  
 313 humidity exchange coefficient  $C_{E10}$  and the ratio  $C_{E10}/C_{D10}$  (or  $C_{k10}/C_{D10}$ )  
 314 as a function of the 10 m wind speed  $U_{10}$ . The reduction in the drag shows  
 315 good agreement with the reduction in  $C_D$  indicated by observational data. The  
 316 friction velocity levels off at very high wind speeds. The value for  $C_{E10}/C_{D10}$   
 317 is in fair agreement with the experimental results presented by Zhang et al.  
 318 (2008) (see Section 1) and is in good agreement with the range of 1.2–1.5  
 319 proposed by Emanuel (1995) for higher wind speeds.

## 320 2.2. SIMULATIONS

321 The tropical cyclones Ivan (2004) and Katrina (2005) in the Gulf of Mex-  
322 ico were simulated with the NWP model HiRLAM. The model grid has a  
323 horizontal resolution of  $0.05^\circ$  and 40 levels in the vertical. The height of the  
324 lowest model level is approximately 30 metres. The wind speed at 10 m height  
325 is obtained through the logarithmic wind profile with eq. (11). HiRLAM uses  
326 a semi-Lagrangian discretization scheme for solving the primitive equations  
327 on all vertical levels, in which a dynamics time step of 2 minutes was used.  
328 The model uses a convective parametrization scheme. Lateral boundary condi-  
329 tions for the HiRLAM simulations were taken from the European Centre  
330 (ECMWF) model archive. The same model version and model grid were used  
331 as by Zweers et al. (2010), which allows for a fair comparison with results  
332 from that study.

333 Forecasts were performed with HiRLAM with model analyses every next  
334 six hours. These 6-hourly analyses are based on every previous forecast and  
335 the assimilation of observational data in a 3D-VAR assimilation scheme.  
336 These simulations were performed for the period 25–30 August 2005 (Ka-  
337 trina) and 11–17 September 2004 (Ivan).

338 For  $z_*$  a value of 0.014 was used. It was verified that the values of  $C_D$  and  
339  $C_k$  at very high wind speeds are not sensitive to this value (*not shown here*).  
340 Therefore, the results are not expected to be very sensitive to the choice for  $z_*$ .  
341 Next to this, we used a value of 1.0 for the turbulent Prandtl number  $Pr_t$ . This  
342 parameter, which describes the difference in turbulent transfers of momentum  
343 and sensible heat, shows to be particularly dependent on stability. Grachev  
344 et al. (2007) refer to several different studies on  $Pr_t$  that indicate that its value  
345 should be around 1.0. Grachev et al. (2007) mention that ‘on average’ the  
346 value for  $Pr_t$  decreases with increasing stability and that  $Pr_t < 1.0$  in the very  
347 stable case. Based on their analysis of the SHEBA (Surface Heat Budget of  
348 the Arctic Ocean) experiment, they also conclude that this is “not a general  
349 result” for the MABL and they show that a value of 1.0 is a proper choice.  
350 Hence, for simplicity we use  $Pr_t = 1.0$ .

351 Finally, an important aspect of the model setup is how sea surface tem-  
352 peratures (SSTs) are prescribed to the NWP model. In the HiRLAM surface  
353 analyses SST fields from the ECMWF model archive are used. The default  
354 approach in HiRLAM, as in many other NWP models, is that during the  
355 forecasts these SSTs are used. In other words, the SSTs are fixed during the  
356 model forecasts and new SSTs are applied every next six hours. This approach  
357 is here the reference scenario, referred to as ‘default SSTs’.

358 The approach described above is generally accepted a valid method for  
359 forecasting ‘normal’ weather conditions, as SSTs then usually do not rapidly  
360 change on local and small scales. Tropical cyclones cause a reduction in SSTs  
361 due to upwelling, currents generated in the ocean upper layer and because

362 of heat uptake from the ocean. This reduction considerably affects the air-  
 363 sea enthalpy flux. Cione and Uhlhorn (2003) mention differences between  
 364 inner-core and ambient SSTs of 0–2 K and further state that SST changes on  
 365 the order of 1 K lead to surface enthalpy flux changes of 40% or more with  
 366 respect to the scenario in which SSTs do not change. D’Asaro et al. (2007)  
 367 come to a similar conclusion: studying Category 4 tropical cyclone Frances  
 368 (2004), they find a decrease in the strongest winds by about  $5 \text{ m s}^{-1}$  to a  
 369 measured wind speed of  $60 \text{ m s}^{-1}$  due to a 0.4 K reduction in the SSTs under  
 370 the storm core.

371 Higher wind speeds would intuitively result in tropical cyclone forecasts  
 372 when the SSTs are overestimated. A ‘compensation’ for this increase in the  
 373 wind speed will result if in the NWP model  $C_H$  is not very large (see eq. (2)).  
 374 Hence, an overestimation of the SSTs could partially explain why Zweers  
 375 et al. (2010) obtain such positive results with  $C_H/C_D$  below Emanuel’s critical  
 376 value of 0.75, despite the use of reduced  $C_D$ .

377 In the default SSTs approach described above new SSTs result from the  
 378 surface analyses every next six hours. In these analyses the NWP model is  
 379 not able to resolve the small scale SST reductions. For reasons described  
 380 above, a second scenario is investigated in which SSTs under the tropical  
 381 cyclones are subject to a simplified parametrized cooling. The aim was not  
 382 to model SST reductions as accurate as possible, but simply to prevent an  
 383 overestimation in the SSTs during the forecasts and to examine the impact of  
 384 the parametrizations in the case that such a simplified SST cooling is applied.  
 385 To that end, an SST reduction was imposed in a sea grid point, if in that  
 386 grid point the 10 m wind speed is in the hurricane wind speed regime, i.e.  
 387 if  $U_{10} > 33 \text{ m s}^{-1}$ . Considering a total cooling of 2.0 K under the tropical  
 388 cyclones (see Cione and Uhlhorn (2003)), a reduction  $\delta T_0$  is applied every  
 389 time step in the model simulation. Estimating the translation speed of the  
 390 tropical cyclones from the experiments with default SSTs, the time interval in  
 391 which they pass a model grid point was estimated to 12 hours. Therefore, we  
 392 use  $\delta T_0 = (2 \text{ K}/12 \text{ hrs}) = 4.63 \times 10^{-5} \text{ K s}^{-1}$ . Thus, in this approach, referred  
 393 to as ‘reduced SSTs’, the SSTs are determined by the ECMWF fields, the  
 394 HiRLAM surface analyses, and additionally by the imposed SST reduction.

### 395 3. Results

#### 396 3.1. DEFAULT SSTS

397 Figure 2 shows the modelled maximum wind speed ( $U_{10_{max}}$ ) and the central  
 398 pressure, and observed wind speed and pressure as described in the National  
 399 Hurricane Center (NHC) tropical cyclone reports Stewart (2004) (Ivan) and  
 400 Knabb et al. (2005) (Katrina). The NWP model overestimates the intensity

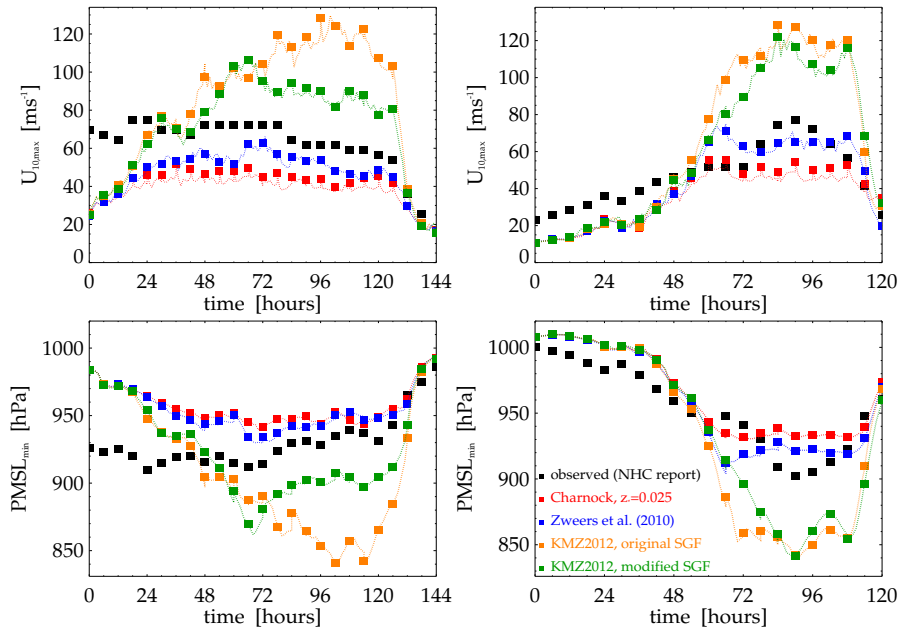


Figure 2. Maximum 10 m wind speed (top) and central pressure (bottom) for tropical cyclones Ivan (left) and Katrina (right). Results obtained with HiRLAM with the new parametrizations in orange (SGF from KMZ2012) and green (modified SGF, *see text*). Results from Zweers et al. (2010) are in red (Charnock's relation,  $z_* = 0.025$ ) and dark blue (their  $C_{D10}$ ).  $t = 0$  corresponds to 11 September 2004 0000 UTC (Ivan) and 25 August 2005 0000 UTC (Katrina). HiRLAM analyses are indicated by squares; observations from Stewart (2004) and Knabb et al. (2005) are in black.

401 with the drag and enthalpy exchange coefficients for both tropical cyclones  
 402 (Figure 2, green lines). During Ivan wind speeds of about  $100 \text{ m s}^{-1}$  are  
 403 modelled, compared to observed wind speeds of  $\simeq 70\text{--}75 \text{ m s}^{-1}$ . The central  
 404 pressure is approximately 870 hPa, compared to the measured value of around  
 405 915 hPa. The intensity drops to a rather constant  $80\text{--}90 \text{ m s}^{-1}$  and central  
 406 pressure of 900 hPa during the simulation, while observed wind speeds were  
 407  $60\text{--}70 \text{ m s}^{-1}$  and the central pressure increased from about 925 to 935 hPa.

408 The differences between observed and modelled intensities are larger for  
 409 Katrina than for Ivan. Knabb et al. (2005) report wind speeds up to  $77 \text{ m s}^{-1}$ ,  
 410 while the modelled wind speeds reach unrealistic values up to about  
 411  $120 \text{ m s}^{-1}$ . This is mainly due to the fact that the model does not reproduce  
 412 the observed collapse of the eyewall (see Figure 2, *time*  $\simeq 48\text{--}72$  hrs). Rather  
 413 similar behaviour was also found by Zweers et al. (2010). On the other hand,  
 414 keeping the SSTs constant during the forecasts also significantly contributes  
 415 to the fact that wind speeds larger than  $100 \text{ m s}^{-1}$  are obtained (see also  
 416 Section 3.2).

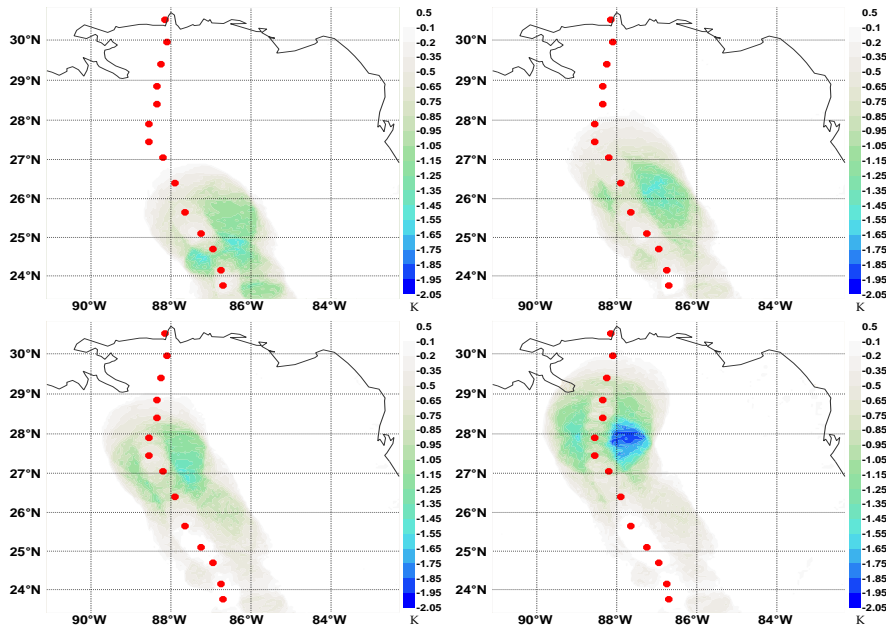


Figure 3. Difference between the SSTs that are kept constant during the forecasts and SSTs that are reduced underneath the cyclones during the forecasts, for tropical cyclone Ivan, at 15 September 2004 at 0600 UTC (top left), 1200 UTC (top right), 1800 UTC (bottom left) and at 16 September 2004 at 0000 UTC (bottom right). The data are from +6h forecasts.

417 As anticipated in advance, the use of the original SGF from KMZ2012  
 418 (see eq. (13)) in the new parametrizations – which leads to a dramatic drop  
 419 in  $C_D$  and decrease in  $u_*$  above  $50 \text{ m s}^{-1}$  – leads to even higher wind speeds  
 420 in the eyewall up to  $130 \text{ m s}^{-1}$  (Figure 2, orange lines). Especially during  
 421 Ivan the differences are very large: the highest wind speeds are larger by  
 422 approximately  $40 \text{ m s}^{-1}$ . This illustrates the significance of the SGF in the  
 423 air-sea exchange parametrizations and shows that a ‘run-away’ effect may  
 424 arise in case of a strong increase in the value of  $C_k/C_D$  at very high wind  
 425 speeds (see Figure 1, orange lines).

### 426 3.2. REDUCED SSTS

427 Figure 3 shows the differences between the perturbed SSTs and the unperturbed  
 428 SSTs at a fixed time during Ivan. As explained in Section 2, in the simu-  
 429 lations with reduced SSTs, these SSTs follow from the archived ECMWF  
 430 SST fields, the HiRLAM surface analyses and the reduction imposed per time  
 431 step, if the wind speed exceeds the imposed criterion (see Section 2.2). Hence,  
 432 the SST reductions shown in Figure 3 are almost, but not exactly, equal to  
 433 the reduction applied in the model. The temperature difference has quite an  
 434 irregular spatial shape, which is due to several reasons. First, the track of the

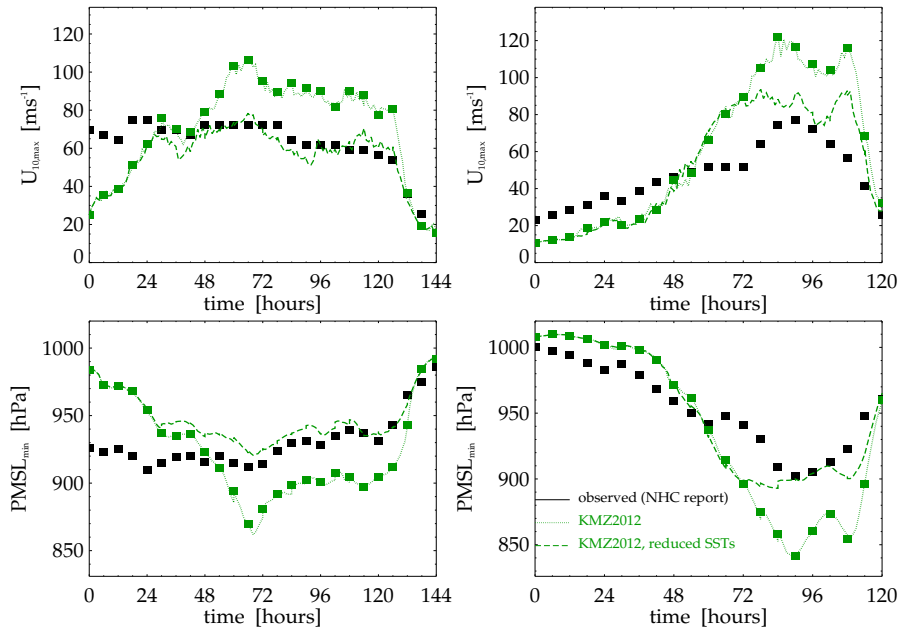


Figure 4. As in Figure 2, but then for the new parametrizations only, with unperturbed SSTs (solid green) and reduced SSTs (dashed green).

435 cyclones is not a straight line. The translation speed is not exactly constant  
 436 during the simulation. Additionally, in model grid points farther away from  
 437 the eye the temperature reduction is smaller than in those locations right under  
 438 the eyewall. Moreover, the wind field is not symmetric.

439 Figure 4 shows the modelled wind speeds and pressure when SSTs are  
 440 reduced in the model. These results are much more realistic. The model pro-  
 441 duces the observed central pressure of 902 hPa during Katrina, while in the  
 442 simulations with default SSTs a value of 840 hPa was obtained. This evidently  
 443 illustrates the impact of the SST modification. During the Category 5 stage  
 444 the modelled wind speeds vary from  $70 \text{ m s}^{-1}$  up to  $90 \text{ m s}^{-1}$ . This is about  
 445  $30 \text{ m s}^{-1}$  lower than the result obtained without the SST modification.

446 The modelled wind speeds during Ivan show very good agreement with  
 447 observed values. Occasionally, the obtained wind speeds are even lower than  
 448 their observed equivalents. Considering the first day in the simulations as  
 449 spin-up, we see that on average the model gives an almost reproduction of  
 450 the observed wind speeds. The central pressure is throughout the entire simu-  
 451 lation slightly too high by 5–10 hPa. The difference with the central pressure  
 452 obtained with (default) unperturbed SSTs varies by about 30–40 hPa.

#### 4. Discussion and conclusions

453

454 The impact of new parametrizations for drag and air-sea enthalpy exchange  
455 on the modelling of tropical cyclone intensity has been examined. These  
456 parametrizations are based on a model that directly accounts for the impact of  
457 spray droplets on the marine atmospheric boundary layer momentum balance.  
458 This model produces a reduction in  $C_D$  at very high wind speeds as in agree-  
459 ment with what measurements indicate. The value for  $C_k/C_D$  is in agreement  
460 with observational data for wind speeds up to  $30 \text{ m s}^{-1}$ . For higher wind  
461 speeds the value for  $C_k/C_D$  is in the favourable range of 1.2–1.5 suggested by  
462 Emanuel (1995).

463 It was shown that the use of the parametrizations in an NWP model leads  
464 to an overestimation of the intensity of the tropical cyclones Ivan (2004) and  
465 Katrina (2005). An important model aspect that relates to this result, which  
466 has been addressed in this paper, is the way in which SSTs are prescribed and  
467 used in the NWP model. Due to strong winds, upwelling and ocean currents,  
468 and the heat uptake by tropical cyclones, the SSTs below tropical cyclones  
469 should reduce. The NWP model that was used, does not resolve these small  
470 scale reductions. In the traditional approach, in which SSTs are kept constant  
471 during forecasts, the winds are overestimated with the model. The application  
472 of a rather simple reduction in the SSTs underneath the cyclones during the  
473 model forecast, of which the magnitude is based on results in other scientific  
474 literature, leads to much better and realistic results. Even good agreement is  
475 found with observed wind speeds and central pressure. This indicates that the  
476 parametrizations may give realistic results for other tropical cyclones as well.  
477 Also, the result supports that  $C_k/C_D \simeq 1.2\text{--}1.5$  at high wind speeds.

478 The sensitivity shown here of eyewall wind speed and central pressure to  
479 the SSTs is in line with results by Cione and Uhlhorn (2003). A decrease in  
480 the SSTs of 1–2 K (see Figure 3) during Ivan leads to a drop in the eyewall  
481 wind speed from about  $90 \text{ m s}^{-1}$  to  $65 \text{ m s}^{-1}$  (see Figure 4). A similar re-  
482 sult is found for Katrina. Regarding this sensitivity to the SSTs, and given  
483 the fact that the result significantly improves when the SSTs are decreased,  
484 the parametrizations are recommended for the modelling of tropical cyclones  
485 with NWP-ocean coupled models.

486 The results are expected not to be very sensitive to the choice for Charnock's  
487 parameter,  $z_*$ . At very high wind speeds  $C_k/C_D$  is not sensitive to  $z_*$  (*not*  
488 *shown here, but verified*). Hence, results obtained with different  $z_*$  are ex-  
489 pected not to be significantly different than shown here. The intensity of the  
490 cyclones is expected to be rather sensitive to the value for the turbulent Prandtl  
491 number,  $Pr_t$ , though. While the value for  $Pr_t$  at very high wind speeds is still  
492 rather uncertain, the impact of the parameter is quite large though (see  $Pr_t$  in  
493 eq. (17)). Using a value larger than 1.0 will result into even better agreement  
494 with observed conditions than found here, although such a value may be

495 considered as rather unrealistic. Application of a value smaller than 1.0 is  
496 realistic, on the contrary, although this will result in (significantly) higher  
497 wind speeds.

498 Compared to Zweers et al. (2010) – who reduced  $C_D$  at high wind speeds  
499 and obtained maximum wind speeds of about  $60 \text{ m s}^{-1}$  (Ivan) and  $70 \text{ m s}^{-1}$   
500 (Katrina) – much higher wind speeds are obtained in the present study. This  
501 is due to the combined effect of the exchange coefficients (see Figure 1). The  
502 behaviour of  $C_k$  is much different and  $C_D$  is larger in Zweers et al. (2010).  
503 In the present study, in the end  $C_k/C_D$  is almost twice as large at  $60 \text{ m s}^{-1}$ .  
504 This illustrates the importance of the value for  $C_k/C_D$  and not simply  $C_k$  or  $C_D$   
505 individually, and explains the much higher wind speeds obtained in this study.  
506 Even with reduced SSTs during the forecasts, which Zweers et al. (2010) did  
507 not consider in their work, the obtained wind speeds are still higher, although  
508 they are realistic.

509 Another study about spray mediated air-sea enthalpy and momentum transfer  
510 is Bao et al. (2011). Their approach is based on a physical mechanism (strati-  
511 fication) different from the direct impact of spray on the momentum balance.  
512 Also different are their use of constant SSTs throughout the entire model  
513 domain ( $T = 302.16 \text{ K}$ ) and the simulation of an idealized tropical cyclone  
514 with their NWP model. The behaviour of  $C_k/C_D$  does show similarities with  
515 our  $C_k/C_D$ , although the values are slightly different:  $C_k/C_D=1.6$  at  $60 \text{ m s}^{-1}$ ,  
516 while our  $C_k/C_D$  is nearly 1.3. They obtain wind speeds up to  $90 \text{ m s}^{-1}$ . Our  
517 simulations with unperturbed SSTs result in even higher wind speeds. This  
518 is partly due to higher SSTs. Our simulations with reduced SSTs result into  
519 wind speeds lower than those obtained by Bao et al. (2011). While the SSTs  
520 are now comparable, our  $C_k/C_D$  is still slightly smaller. The wind speeds  
521 during Katrina are still higher than observed. To a great extent this is due  
522 to the fact that our NWP model is not capable of resolving the collapse of  
523 the eyewall at 27 August 2005 (see Figure 4, *time=48–72hrs*) properly. This  
524 could be due to the fact that our NWP model uses a convective parametriza-  
525 tion scheme. Although very good results for Ivan are obtained, it would be  
526 interesting to see the impact of the parametrizations in a non-hydrostatic  
527 NWP model, as in Bao et al. (2011).

528 Finally, tropical cyclone intensity in NWP models is also sensitive to the  
529 formulation used for the spray generation function (SGF). In the present  
530 study, we anticipated that the drag coefficient becomes too small when the  
531 SGF by Kudryavtsev et al. (2012) is used. It was shown that this results  
532 into unrealistically high wind speeds and extremely low central pressure.  
533 Our modification in the SGF is a step towards the concept that the length  
534 of wave breaking fronts and the amount of white capping should saturate at  
535 very high wind speeds, as is suggested in both theoretical and experimental  
536 studies (see Section 2.1). Although it is a step in the good direction, possi-  
537 bly a stronger limitation to the droplet production is required. To that end,



538 better understanding of wave breaking at very high wind speeds is required.  
539 This could lead to better representation of wave breaking statistics and spray  
540 droplet production from individual breaking crests at very high wind speeds  
541 in models. This should in the end lead to better tropical cyclone forecasts.  
542 Eventually, with climate models indicating that future tropical cyclones will  
543 become more severe Knutson et al. (2010), it becomes more significant to  
544 aim at better understanding (and modelling) of the processes that dominate  
545 the dynamics at the air-sea interface in tropical cyclone conditions.

#### 546 **Acknowledgements**

547 The authors acknowledge the support by the Netherlands Organization for  
548 Scientific Research (NWO), project number 816.01.011, and the Office of  
549 Naval Research (ONR), Grant N000 14-08-1-0609. Vladimir Kudryavtsev  
550 acknowledges support of the Russian Government grant No.11.G34.31.0078.  
551 In addition, the assistance by Toon Moene is much appreciated.

#### 552 **References**

- 553 Andreas, EL (2004), Spray stress revisited. *J. Phys. Oceanogr.* **34**(6), 1429–1440.  
554 Andreas, EL (2011), Fallacies of the Enthalpy Transfer Coefficient over the Ocean in High  
555 Winds. *J Atmos Sci* **68**(7), 1435–1445.  
556 Bao, JW, CW Fairall, SA Michelson, and L Bianco (2011), Parameterizations of sea-spray  
557 impact on the air-sea momentum and heat fluxes. *Mon Weather Rev* **139**(12), 3781–3797.  
558 Bender, MA, I Ginis, R Tuleya, B Thomas, and T Marchok (2007), The operational GFDL  
559 coupled hurricane-ocean prediction system and a summary of its performance. *Mon*  
560 *Weather Rev* **135**(12), 3965–3989.  
561 Bye, JAT and AD Jenkins (2006), Drag coefficient reduction at very high wind speeds. *J*  
562 *Geophys Res* **111**, C03024, doi:10.1029/2005JC003114  
563 Charnock, H. (1955), Wind stress on a water surface. *Q J R Meteorol Soc* **81**(350), 639–640.  
564 Cione, JJ and EW Uhlhorn (2003), Sea surface temperature variability in hurricanes:  
565 Implications with respect to intensity change. *Mon Weather Rev* **131**(8), 1783–1796.  
566 D’Asaro, EA, TB Sanford, PP Niiler, and EJ Terrill (2007), Cold wake of Hurricane Frances.  
567 *Geophys Res Lett* **34**, L15609, doi:10.1029/2007GL030160  
568 Drennan, WM, JA Zhang, JR French, C McCormick, and PG Black (2007), Turbulent fluxes  
569 in the hurricane boundary layer. Part II: Latent heat flux. *J Atmos Sci* **64**(4), 1103–1115.  
570 Emanuel, KA (1986), An air-sea interaction theory for tropical cyclones. Part 1: Steady-state  
571 maintenance. *J Atmos Sci* **43**(6), 585–604.  
572 Emanuel, KA (1995), Sensitivity of tropical cyclones to surface exchange coefficients and a  
573 revised steady-state model incorporating eye dynamics. *J Atmos Sci* **52**(22), 3969–3976.  
574 French, JR, WM Drennan, JA Zhang, and PG Black (2007), Turbulent fluxes in the hurricane  
575 boundary layer. Part I: Momentum flux. *J Atmos Sci* **64**(4), 1089–1102.  
576 Garratt, JR (1992), *The Atmospheric Boundary Layer*. Cambridge Univ Pr, 316 pp.  
577 Grachev, AA, EL Andreas, CW Fairall, PS Guest, and POG Persson (2007), On the turbu-  
578 lent Prandtl number in the stable atmospheric boundary layer. *Boundary-Layer Meteorol*  
579 **125**(2), 329–341

- 580 Holthuijsen, LH, MD Powell, and JD Pietrzak (2012), Wind and Waves in extreme hurricanes.  
581 *J Geophys Res* **117**, C09003, doi:10.1029/2012JC007983
- 582 Jarosz, E, DA Mitchell, DW Wang, and WJ Teague (2007), Bottom-up determination of air-sea  
583 momentum exchange under a major tropical cyclone. *Science* **315**(5819), 1707.
- 584 Knabb, RD, JR Rhome, and DP Brown (2005), Tropical Cyclone Report Hurricane  
585 Katrina. Technical report, NHC, 43 pp, URL: [http://www.nhc.noaa.gov/pdf/TCR-](http://www.nhc.noaa.gov/pdf/TCR-AL122005_Katrina.pdf)  
586 [AL122005\\_Katrina.pdf](http://www.nhc.noaa.gov/pdf/TCR-AL122005_Katrina.pdf)
- 587 Knutson, TR, JL McBride, J Chan, KA Emanuel, G Holland, C Landsea, I Held, JP Kossin,  
588 AK Srivastava, and M Sugi (2010), Tropical cyclones and climate change. *Nature*  
589 *Geoscience* **3**, 157–163
- 590 Kudryavtsev, VN (2006), On the effect of sea drops on the atmospheric boundary layer. *J*  
591 *Geophys Res* **111**, C07020, doi:10.1029/2005JC002970
- 592 Kudryavtsev, VN and VK Makin (2009), Model of the spume sea spray generation. *Geophys*  
593 *Res Lett* **36**, L06801, doi:10.1029/2008GL036871
- 594 Kudryavtsev, VN and VK Makin (2011), Impact of Ocean Spray on the Dynamics of the  
595 Marine Atmospheric Boundary Layer. *Boundary-Layer Meteorol* **140**(3), 383–410
- 596 Kudryavtsev, VN, VK Makin, and S Zilitinkevich (2012), On the sea-surface drag and  
597 heat/mass transfer at strong winds. Technical Report WR2012–02, KNMI, 28 pp, URL:  
598 <http://www.knmi.nl/knmi-library/knmipubWR/WR2012-02.pdf>
- 599 Makin, VK (1999), A note on wind speed and sea state dependence of the heat exchange  
600 coefficient. *Boundary-Layer Meteorol* **91**(1), 127–134
- 601 Makin, VK (2005), A note on the drag of the sea surface at hurricane winds. *Boundary-Layer*  
602 *Meteorol* **115**(1), 169–176
- 603 Moon, IJ, I Ginis, T Hara, and B Thomas (2007), A physics-based parameterization of air-  
604 sea momentum flux at high wind speeds and its impact on hurricane intensity predictions.  
605 *Mon Weather Rev* **135**(8), 2869–2878
- 606 Phillips, OM (1985), Spectral and statistical properties of the equilibrium range in wind-  
607 generated gravity waves. *J Fluid Mech* **156**(1), 505–31
- 608 Powell, MD, PJ Vickery, and TA Reinhold (2003), Reduced drag coefficient for high wind  
609 speeds in tropical cyclones. *Nature* **422**(6929), 279–283
- 610 Rastigejev, Y, SA Suslov, and YL Lin (2011), Effect of ocean spray on vertical momentum  
611 transport under high-wind conditions. *Boundary-Layer Meteorol* **141**(1), 1–20
- 612 Richter, DH and PP Sullivan (2013), Sea surface drag and the role of spray. *Geophys Res Lett*  
613 **40**(3) 656–660, doi:10.1002/grl.50163.
- 614 Smith, RK, and MT Montgomery (2012), On the existence of the logarithmic surface layer in  
615 the inner core of hurricanes. *Q J R Meteorol Soc* **140** 72–81, DOI:10.1002/qj.2121.
- 616 Stewart, SR (2004), Tropical Cyclone Report Hurricane Ivan. Technical Report, NHC, 44 pp,  
617 URL: [http://www.nhc.noaa.gov/pdf/TCR-AL092004\\_Ivan.pdf](http://www.nhc.noaa.gov/pdf/TCR-AL092004_Ivan.pdf)
- 618 Zhang, JA, PG Black, JR French, and WM Drennan (2008), First direct measurements of  
619 enthalpy flux in the hurricane boundary layer: The CBLAST results. *Geophys Res Lett*  
620 **35**, L14813, doi:10.1029/2008GL034374
- 621 Zweers, NC, VK Makin, JW de Vries, and G Burgers (2010), A sea drag relation for hurricane  
622 wind speeds. *Geophys Res Lett* **37**, L21811, doi:10.1029/2010GL045002